

BBC

ENGINEERING DIVISION

MONOGRAPH

NUMBER 17: APRIL 1958

The Design of a Linear Phase-Shift Low-pass Filter

by

L. E. WEAVER, B.Sc.

(Designs Department, BBC Engineering Division)

BRITISH BROADCASTING CORPORATION

PRICE FIVE SHILLINGS



BBC ENGINEERING MONOGRAPH

No. 17

THE DESIGN OF A LINEAR PHASE-SHIFT LOW-PASS FILTER

by

L. E. Weaver, B.Sc.

(DESIGNS DEPARTMENT, BBC ENGINEERING DIVISION)

APRIL 1958

BRITISH BROADCASTING CORPORATION

FOREWORD

THIS is one of a series of Engineering Monographs published by the British Broadcasting Corporation. About six are produced every year, each dealing with a technical subject within the field of television and sound broadcasting. Each Monograph describes work that has been done by the Engineering Division of the BBC and includes, where appropriate, a survey of earlier work on the same subject. From time to time the series may include selected reprints of articles by BBC authors that have appeared in technical journals. Papers dealing with general engineering developments in broadcasting may also be included occasionally.

This series should be of interest and value to engineers engaged in the fields of broadcasting and of telecommunications generally.

Individual copies cost 5s. post free, while the annual subscription is £1 post free. Orders can be placed with newsagents and booksellers, or BBC PUBLICATIONS, 35 MARYLEBONE HIGH STREET, LONDON, W.1.

CONTENTS

<i>Section</i>	<i>Title</i>	<i>Page</i>
	PREVIOUS ISSUES IN THIS SERIES	4
	SUMMARY	5
1.	INTRODUCTION	5
1.1.	Specification	5
2.	METHOD OF DESIGN	6
2.1.	Choice of Design Method	6
2.2.	Theory	6
2.3.	Determination of Numerical Constants	8
2.4.	Lattice Arms	9
2.5.	Impedance Function	11
3.	REDUCTION TO UNBALANCED FORM	11
3.1.	General	11
3.2.	Theory of Reduction to Ladder Form	12
3.3.	Reduction Process	12
3.4.	Calculation of Element Values	15
4.	PRACTICAL CONSIDERATIONS	16
4.1.	Components	16
4.2.	Mechanical	18
4.3.	Alignment	18
4.4.	Resistance Compensation	20
4.5.	Improvement of Group-Delay Characteristic	20
5.	REFERENCES	21
	<hr/>	
	NOTE ON RANDOM FLUCTUATION NOISE IN IMAGE ORTHICON CAMERA TUBES	22

PREVIOUS ISSUES IN THIS SERIES

No.	Title	Date
1.	<i>The Suppressed Frame System of Telerecording</i>	JUNE 1955
2.	<i>Absolute Measurements in Magnetic Recording</i>	SEPTEMBER 1955
3.	<i>The Visibility of Noise in Television</i>	OCTOBER 1955
4.	<i>The Design of a Ribbon Type Pressure-gradient Microphone for Broadcast Transmission</i>	DECEMBER 1955
5.	<i>Reproducing Equipment for Fine-groove Records</i>	FEBRUARY 1956
6.	<i>A V.H.F./U.H.F. Field-strength Recording Receiver using Post-detector Selectivity</i>	APRIL 1956
7.	<i>The Design of a High Quality Commentator's Microphone Insensitive to Ambient Noise</i>	JUNE 1956
8.	<i>An Automatic Integrator for Determining the Mean Spherical Response of Loudspeakers and Microphones</i>	AUGUST 1956
9.	<i>The Application of Phase-coherent Detection and Correlation Methods to Room Acoustics</i>	NOVEMBER 1956
10.	<i>An Automatic System for Synchronizing Sound on Quarter-inch Magnetic Tape with Action on 35-mm. Cinematograph Film</i>	JANUARY 1957
11.	<i>Engineering Training in the BBC</i>	MARCH 1957
12.	<i>An Improved 'Roving Eye'</i>	APRIL 1957
13.	<i>The BBC Riverside Television Studios: The Architectural Aspects</i>	JULY 1957
14.	<i>The BBC Riverside Television Studios: Some Aspects of Technical Planning and Equipment</i>	OCTOBER 1957
15.	<i>New Equipment and Methods for the Evaluation of the Performance of Lenses for Television</i>	DECEMBER 1957
16.	<i>Analysis and Measurement of Programme Levels</i>	MARCH 1958

SUMMARY

This Monograph describes the theoretical and practical details of the design of a very linear phase-shift low-pass filter intended to remove noise and other irrelevant information above approximately 3 Mc/s from the output of a television camera control unit.

The problem was to design a low-pass filter which could be inserted in a video circuit—in particular the output of a camera control unit—to limit the band to a little above 3 Mc/s with the absolute minimum of distortion. For this purpose it was essential that the filter should be in unbalanced form and a detailed description of the process of reduction from the original lattice network is given.

In the filter described, the pass-band is flat within ± 0.1 dB to 3 Mc/s and the group-delay characteristic varies over a range of only ± 10 m μ s throughout the pass-band and well into the attenuating region. The practical filter was made to conform more closely with the calculated characteristics than is usually possible, by the application of resistance compensation for the dissipation of the circuit elements.

The filter has an impedance of 75 ohms and is economical, both in the number of circuit elements employed and in the space needed for mounting, since it measures only 6 in. by $2\frac{11}{16}$ in. by $2\frac{13}{16}$ in. overall, exclusive of fixing lugs.

A short section of the Monograph is devoted to a description of the method of checking such a filter by sine-squared pulses, and shows how this technique makes it possible to improve somewhat its already very linear group-delay characteristic.

THE DESIGN OF A LINEAR PHASE-SHIFT LOW-PASS FILTER

1. Introduction

Since the video band finally transmitted in the British 405-line television system is approximately 3 Mc/s wide, any signal above that frequency which is produced by a camera can be considered as unnecessary and irrelevant. Furthermore, if allowed to remain, such signals may undergo intermodulation during subsequent non-linear processes, such as gamma correction, and appear as noise in the final video band.

It was considered desirable, therefore, to investigate the possibility of designing and constructing a low-pass filter which could be connected in the video output of a camera control unit and which would limit the band to a little above 3 Mc/s whilst introducing only the absolute minimum of distortion. The resulting filter forms the subject of this Monograph.

The extremely small amount of transient distortion introduced by the filter is clearly indicated in the photographs forming Figs. 13 and 14 which show the '2 T' and 'T' sine-squared pulses before and after transmission through it. The linearity of the phase response in the neighbourhood of the cut-off frequency is clearly demonstrated by the symmetry of the response to the 'T' pulse, which has frequency components extending up to 6 Mc/s.

A photograph of the filter with the lid of the screening can removed to show the construction forms Fig. 12, whilst Fig. 11 shows the method of mounting the components.

1.1 Specification

The requirement of very low distortion means, first of all, that the variations in loss and group delay over the

pass-band must be kept extremely small to avoid corresponding deformations being produced in the transmitted waveform. Above 3 Mc/s it would seem desirable, from the point of view of band limiting, to have the filter cut-off as rapidly as possible. However, too rapid a cut-off is undesirable for two reasons: firstly, the difficulty of obtaining linear phase increases very rapidly as the cut-off slope increases, and, secondly, severe 'ringing' may be seen on certain special pictures such as Test Card 'C' which contain an unusually high amount of energy at and even somewhat beyond 3 Mc/s.

On a basis of previous experience, the following tentative specification was drawn up as a target:

- (a) The insertion loss between 75-ohm terminations should be flat within ± 0.1 dB from zero frequency to 3 Mc/s. The loss may increase slightly up to 3.4 Mc/s, and should thereafter increase as quickly as possible.
- (b) The insertion group-delay should be constant within ± 20 m μ s up to 3 Mc/s, after which the tolerance may be relaxed progressively, say roughly in proportion to the increasing loss.
- (c) The filter impedance should be as close as possible to 75 ohms over as great a range of the pass-band as possible.
- (d) The least possible number of filter elements should be used consistent with a good performance in order to keep down the physical size and cost, and they should have values such that they are not difficult to manufacture or purchase. In addition, the filter as a whole should be easy to manufacture and align, and stable in its characteristics.

Requirements (a) and (b), although necessarily in steady-state terms because the filter is designed on that

curve π/a , as it is in the pass-band. The argument does not show where the cut-off frequency f_c is to be located within the interval BC, so for reasons of symmetry we shall put it at the centre of the interval, obtaining what Bode and Dietzold call a 'three-quarter spaced cut-off'; this location can, in fact, be justified analytically.

It may be objected that no consideration has been given above to the reflection effects which must occur in the region of the cut-off frequency. However, the mean slope of the phase-shift curve is not changed due to the reflections over the interval BC, since the total increment in phase is not altered, but the shape of the curve is modified. If linearity of phase over the cut-off interval is important, it is necessary to take account of these reflections, either explicitly or implicitly, in the design of the filter. This point will be dealt with again later.

Although the above argument has been based upon a low-pass filter, it applies equally well to the band-pass case and also, over a restricted frequency range, to a high-pass filter.

2.3 Determination of Numerical Constants

It is known from classical filter theory that if the arms of a symmetrical lattice network have impedances Z_x and Z_y , then the image transfer constant is given by

$$\tanh \frac{\theta}{2} = \sqrt{\frac{Z_x}{Z_y}} \dots \dots \dots (1)$$

and the image impedance Z_I by

$$Z_I = \sqrt{Z_x Z_y} \dots \dots \dots (2)$$

It is also known that, by Foster's Reactance Theorem, the impedance of the arms may be written

$$Z_x = K_x \times jf \times \frac{a_2 a_4 \dots a_{c-2} a_c a_{c+2} \dots a_n}{a_1 a_3 \dots a_{c-1} a_{c+1} \dots a_{n-1}} \dots \dots (3)$$

$$Z_y = \frac{K_y}{jf} \times \frac{a_1 a_3 \dots a_{c-1} a_{c+1} \dots a_n}{a_2 a_4 \dots a_{c-2} a_{c+2} \dots a_{n-1}} \dots \dots (4)$$

where the a 's are terms of the form $1 - \left(\frac{f}{f_r}\right)^2$ and K_x and K_y are numerical constants.

$$\therefore \tanh \frac{\theta}{2} = jf \sqrt{\frac{K_x}{K_y}} \times \frac{a_2 a_4 \dots a_{c-2}}{a_1 a_3 \dots a_{c-1}} \sqrt{a_c} \dots \dots (5)$$

and
$$Z_I = \sqrt{K_x K_y} \times \frac{a_{c+2} a_{c+4} \dots a_n}{a_{c+1} a_{c+3} \dots a_{n-1}} \sqrt{a_c} \dots \dots (6)$$

Obviously, although one particular scheme of critical frequencies has been selected in setting up equations (3) and (4), the argument is perfectly general. It is immaterial whether Z_x has a pole or a zero at zero and infinite frequencies, and the cut-off factor a_c may also be either a zero, as shown, or a pole. Furthermore, Z_x and Z_y may be interchanged with only the consequence, trivial for the

present purpose, of a phase-reversal of the signal transmitted by the network.

An important point which now arises is the determination of the values of K_x and K_y , without which the reactance arms of the network cannot be stated.

The value of the product $K_x K_y$ is known from equation (6). At zero frequency the a 's become unity and

$$Z_{I0}^2 = K_x K_y \dots \dots \dots (7)$$

where Z_{I0} is the zero frequency impedance of the network.

If the value of K_x/K_y can also be found, then each is known separately. Bode and Dietzold do this in the following manner. Considering the pass-band only, and assuming perfect termination, the linear-phase requirement can be formulated analytically as

$$\tanh \frac{\theta}{2} = \tanh \frac{j\pi f}{2a} = j \tan \frac{\pi f}{2a} \dots \dots \dots (8)$$

But from the continued product expansions of the sine and cosine of an angle,

$$j \tan \frac{\pi f}{2a} = \frac{j\pi f}{2a} \times \frac{b_2 b_4 b_6 \dots b_n}{b_1 b_3 b_5 \dots b_{n-1}} \dots \dots \dots (9)$$

where

$$b_r = 1 - \left(\frac{f}{ra}\right)^2$$

Then, for frequencies in the pass range only and ignoring all else, equations (5) and (9) are identical so that corresponding terms can be identified, giving

$$\sqrt{\frac{K_x}{K_y}} = \frac{\pi}{2a} \dots \dots \dots (10)$$

This particular value of multiplying constant ensures the optimum degree of linearity of phase-shift within the pass-band region, but it may be modified to effect some desired compromise between stop-band attenuation and phase linearity.

A perhaps less elegant but more general method for deriving the value of the ratio $\frac{K_x}{K_y}$ is the following. Near zero frequency the image phase constant is identical with the insertion phase shift, since the filter is ideally matched. Consequently the value of the group-delay at zero frequency can be obtained from equation (5), and the linear-phase condition is imposed by equating this to the mean delay of the filter which in this case, as is evident from

Fig. 2, is equal to $\frac{\pi}{2\pi a} = \frac{1}{2a}$.

The mathematics can be simplified at the expense of a little rigour. In the close neighbourhood of zero frequency the a 's in equation (5) are unity and their rate of change is very small, so that the term containing them is itself unity. Also, the phase angle is so small that θ may be put for $\tan \theta$, and equation (5) becomes

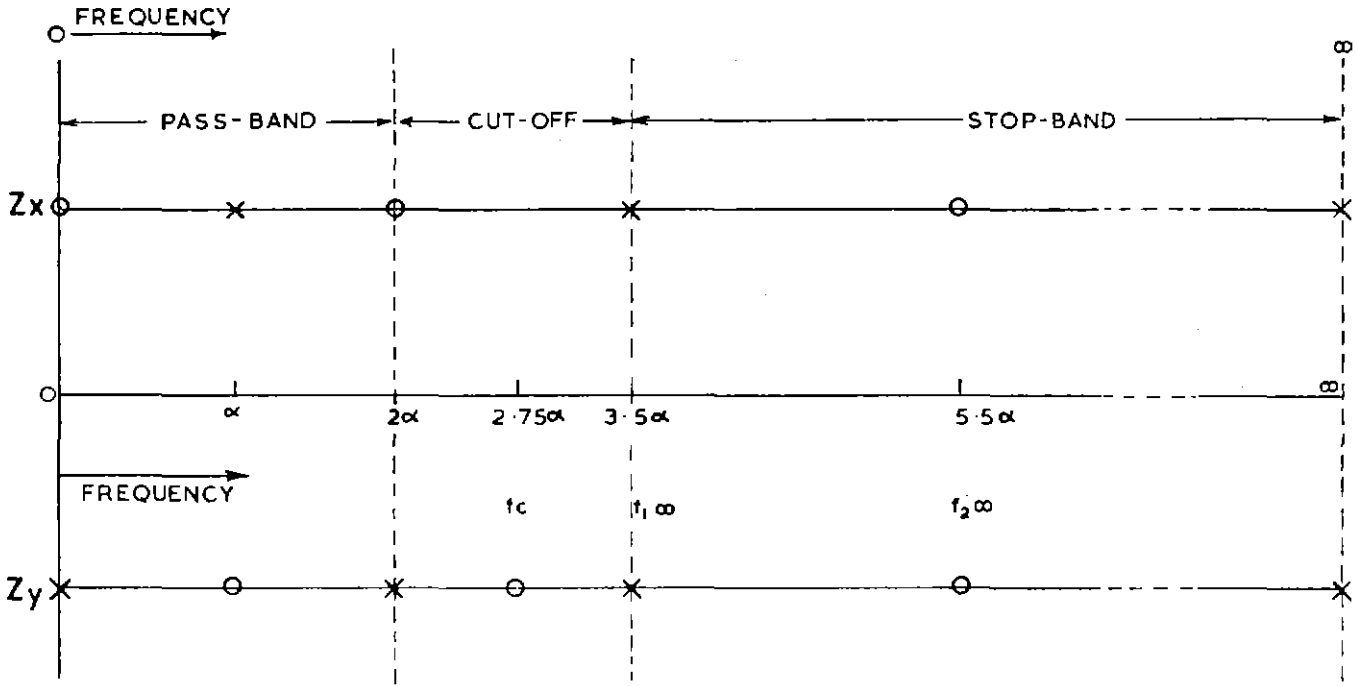


Fig. 3 — Critical-frequency scheme for linear-phase low-pass filter

$$\frac{\theta}{2} = f \sqrt{\frac{K_x}{K_y}} \text{ for } f \rightarrow 0 \dots\dots\dots (5a)$$

From this the group delay at zero frequency is

$$\left[\frac{d\theta}{d\omega} \right]_{f \rightarrow 0} = \frac{1}{\pi} \sqrt{\frac{K_x}{K_y}},$$

and when it is equated to the mean delay $\frac{1}{2a}$ the result

$$\sqrt{\frac{K_x}{K_y}} = \frac{\pi}{2a} \text{ is obtained as in equation (10).}$$

The latter method is not restricted to low-pass filters and may be applied to other types. For example a band-pass filter can have the linear-phase condition applied at the mid-band frequency, and correspondingly for other types.

2.4 Lattice Arms

Two things remain to be decided before the precise forms of the lattice arms can be settled, the number of critical frequencies within the pass-band and the number of critical frequencies in the stop-band.

In each case the minimum number which makes the filter satisfy the required conditions will be used in order to keep the total of reactive elements as small as possible.

An increase in the number of critical frequencies in the pass-band has the result of improving the linearity of the

phase response over the region where the impedance is good enough for reflection effects to be negligible, and also increases the sharpness of cut-off by reducing the width of the transition region in the neighbourhood of the cut-off. The magnitude of the stop-band loss is very little affected.

The number and location of the critical frequencies in the stop-band not only influence the magnitude of the loss in that region but also the linearity of the phase response in the cut-off region. Equation (6) makes it clear that the network impedance up to the cut-off frequency is resistive, but varies with frequency in a manner which depends upon the cut-off factor a_c and terms which are functions only of the locations of the critical frequencies in the stop-band. The consequent reflection effects over the upper part of the pass-band very appreciably modify the phase and amplitude characteristics compared with those for image terminations.

On the basis of previous experience, it was estimated that two critical frequencies in the pass-band and two in the stop-band would probably meet the requirements of Section 1.1. The scheme shown in Fig. 3 could then be drawn up and from it the values of the reactance arms could be written down as

$$Z_x = \frac{\pi}{2a} \times jf \times \frac{\left[1 - \left(\frac{f}{2\alpha} \right)^2 \right] \left[1 - \left(\frac{f}{5.5\alpha} \right)^2 \right]}{\left[1 - \left(\frac{f}{\alpha} \right)^2 \right] \left[1 - \left(\frac{f}{3.5\alpha} \right)^2 \right]} \dots (11)$$

$Z_y =$

$$\frac{2a}{\pi} \times \frac{1}{jf} \times \frac{\left[1 - \left(\frac{f}{a}\right)^2\right] \left[1 - \left(\frac{f}{2.75a}\right)^2\right] \left[1 - \left(\frac{f}{5.5a}\right)^2\right]}{\left[1 - \left(\frac{f}{2a}\right)^2\right] \left[1 - \left(\frac{f}{3.5a}\right)^2\right]} \dots \dots \dots (12)$$

if it is supposed, for simplicity, that Z_i equals unity.

The double spacing between the critical frequencies at $3.5a$ and $5.5a$ follows a suggestion by Bode and Dietzold that the infinite series of critical frequencies which should ideally be present can be represented by a finite series terminated in this manner. Although the statement is made without proof, in fact it does seem to give a close approximation to the optimum phase response through the cut-off region. Nevertheless, this spacing, as well as the cut-off spacing and the values of the numerical constants multiplying the reactance arms, may be modified to suit special requirements.

The expressions (11) and (12) can be put into a more convenient form by using the parameter $x = \frac{f}{2.75a}$, where

$2.75a$ is the cut-off frequency, then

$$Z_x = 4.3197jx \cdot \frac{(1 - 1.8904x^2)(1 - 0.2500x^2)}{(1 - 7.5625x^2)(1 - 0.6172x^2)} \dots (13)$$

$$Z_y = \frac{0.37499}{jx} \cdot \frac{(0.13223 - x^2)(1 - x^2)(4 - x^2)}{(0.52893 - x^2)(1.61983 - x^2)} \dots (14)$$

From these equations the insertion loss and phase-shift functions can be calculated from the well-known expression which, since Z_x and Z_y refer to a symmetrical lattice of unit impedance, simplifies to

$$\text{Insertion loss} = \frac{(1 + Z_x)(1 + Z_y)}{Z_x - Z_y} \dots \dots \dots (15)$$

The resulting curves are shown in Fig. 4. It was decided from these that, provided the impedance of the filter were good enough, the requirements originally laid down would be sufficiently well fulfilled with the present configuration and the nominal cut-off frequency made 3.6 Mc/s .

The actual physical forms of the lattice reactance arms can easily be determined from the scheme of critical frequencies given in Fig. 3, or alternatively from equations (13) and (14) which are the same thing expressed analytically.

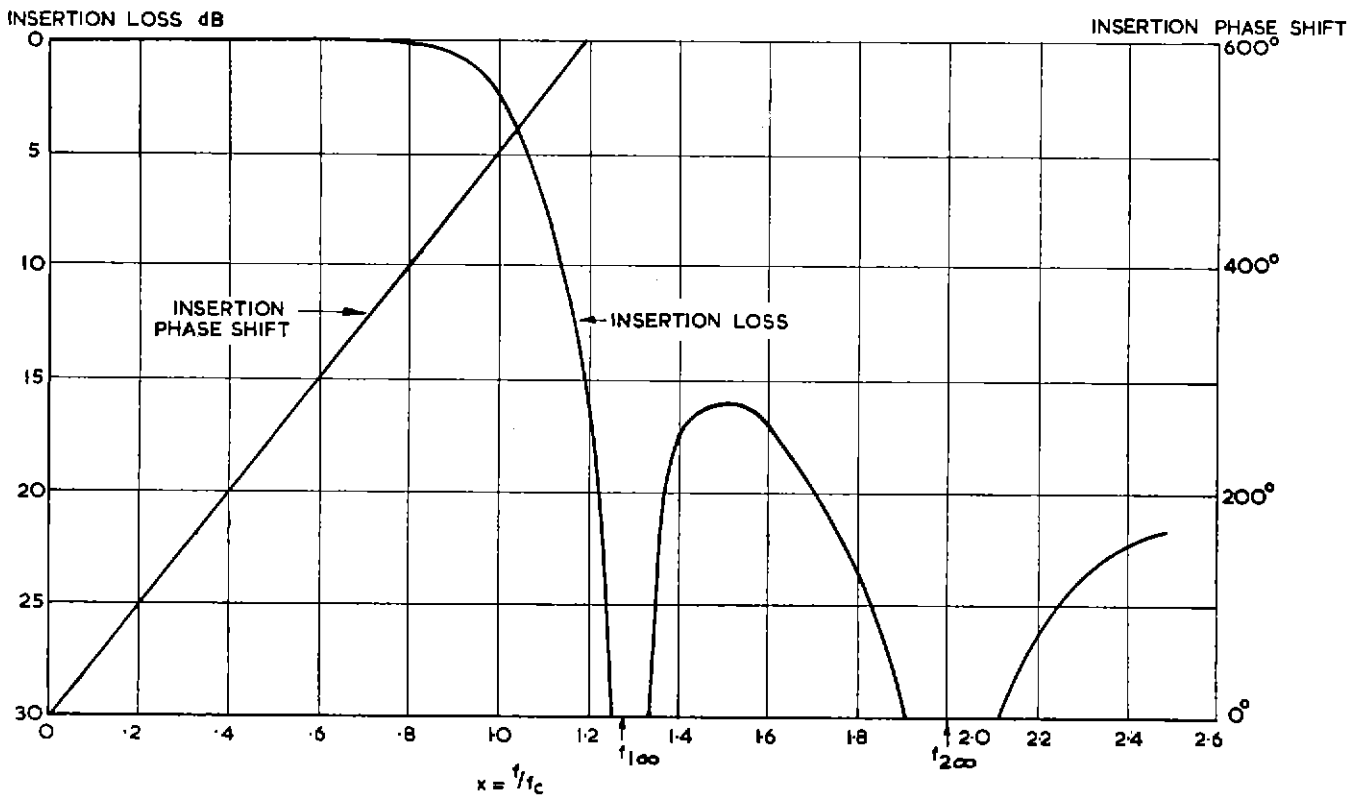


Fig. 4 — Insertion loss and phase shift of linear-phase low-pass filter

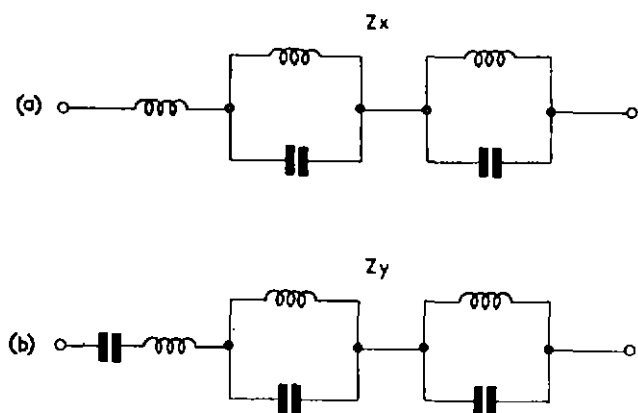


Fig. 5 — Canonical forms of the lattice arms

A convenient canonical form of the generalized two-terminal reactance network has the configuration of a resonant circuit in series with the appropriate number of antiresonant circuits, and a typical argument for applying this to the present case would run as follows:

Z_x has four critical frequencies, excluding zero and infinite frequencies, so that the total number of reactance elements it contains must be one more than this number, that is, five. The arm has a zero at zero frequency, so the series capacitor of the resonant circuit of the canonical arm must be omitted, although the series inductor must still be present because the arm has a pole at infinite frequency. Z_x must therefore consist of an inductor in series with two antiresonant circuits in order to have the requisite five elements, as is shown in Fig. 5(a).

Z_y has five critical frequencies, apart from zero and infinite frequency, and must therefore possess six elements. The pole at zero frequency indicates that the series capacitor of the canonical network must be present; the inductor must also be there because the total number of elements in the arm is even. The configuration, as given in Fig. 5(b), must correspondingly be a resonant circuit in series with two antiresonant circuits.

The actual element values can readily be obtained from (11) and (12), if required, by a process to be given in a later section. It should perhaps be pointed out that in a practical lattice filter the particular configurations of Figs. 5(a) and 5(b) would not necessarily be used unless the element values happened to be suitable. Very often it is necessary to make use of various equivalent circuits to replace parts of the arms until each has been rearranged into the most convenient form for the purpose.

2.5 Impedance Function

The impedance is obtained directly from equations (13) and (14)

$$Z_I = \sqrt{Z_x Z_y} = \frac{1 - 0.2500x^2}{1 - 0.6172x^2} \sqrt{1 - x^2} \dots (16)$$

where, it must be remembered, Z_I has been chosen to be

nominally unity. The variation of impedance with frequency can then be calculated, and is shown in Fig. 6. It resembles the familiar 'm-derived' impedance of the Zobel type sections.

At 3 Mc/s $x = \frac{3 \cdot 0}{3 \cdot 6} = 0.833$, and from the curve $Z_I = 0.80$ approximately at this value of x . The return loss at 3 Mc/s is therefore $20 \log_{10} \frac{1 \cdot 80}{0 \cdot 20} = 19.5$ dB, and increases rapidly as the frequency decreases. When the decrease of mean energy with increasing frequency in the video signal is taken into account, it is apparent that an impedance of this type is quite adequate for most purposes from the point of view of reflections into other apparatus. All the same, the filter must be properly terminated in order to achieve the intended response for the reason given in the previous section.

3. Reduction to Unbalanced Form

3.1 General

There is no doubt that balanced networks cannot, in general, be tolerated in video circuits. The economic reason is that the number of reactive elements is immediately doubled as compared with the unbalanced form and more than double the care is required in the initial setting-up due to the need for maintaining the balance of the lattice bridge. In addition, except for a number of relatively short links, video circuits are unbalanced and transformers are not really practicable for conversion from unbalanced to balanced forms and vice versa to allow the lattice network to be inserted.

Since, as has already been mentioned, the linear-phase filters of Bode and Dietzold cannot be completely reduced to the ladder form, two main courses are available:

- (a) Conversion of the filter into one or more bridged-T sections. Inspection of equation (15) shows that the solution of $Z_x - Z_y = 0$ gives all frequencies, real or imaginary, at which the loss is infinite. Each pair of complex conjugate roots can be assigned to an individual simpler filter section of the same impedance and having real element values in the bridged-T form, and the filter is reconstructed as a chain of these simpler sections.^(3, 4)

This process is somewhat tedious but not difficult, and has the merit of giving elements with real, if not always convenient, element values by means of a direct algebraic process. Unfortunately, the sections so produced must in general be realized as bridged-T networks, since ladder equivalents are not available. One great inconvenience with this form is the difficulty of maintaining the impedance of each section correct over the entire frequency range due to the inevitable stray reactances, as well as to the difficulties experienced with the coupling and balance of the transformer which has to be used to form the bridged-T.

RELATIVE ZI

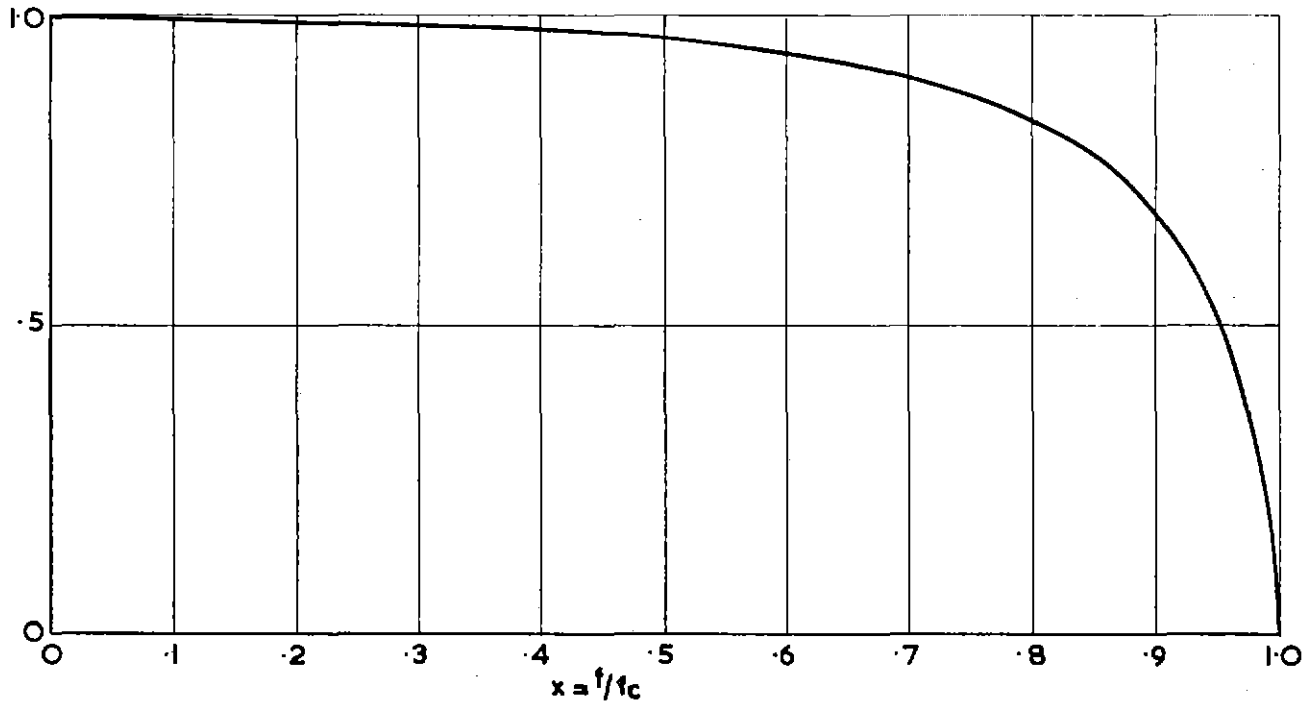


Fig. 6 — Relative impedance of linear-phase low-pass filter

The consequence of these mismatches occurring between sections having relatively large time delays is a series of reflections which seriously upset the flatness of the loss and phase responses. Various devices can be brought into use to minimize these effects, but as a rule a considerable amount of care and attention has to be given to the alignment of the complete network in order to obtain a really satisfactory result.

- (b) The second method uses a step-by-step reduction of the original filter to ladder form. This process is continued until an irreducible minimum is left which is then converted into a bridged-T section, and its success largely depends upon the possibility of taking the reduction sufficiently far to make the bridged-T section relatively simple.

The process is usually fairly lengthy and tedious, but, when it can be carried out in such a manner as to give elements with convenient magnitudes, the result is a filter containing only one transformer which is hardly any more difficult to align than a conventional Zobel type. This solution, where the main burden is carried by the designer rather than the tester, is considered to be the better engineering approach and was accordingly adopted in the present case.

3.2 Theory of Reduction to Ladder Form

The relevant equivalent circuits are given in Figs. 7(a), 7(b), and 7(c). These are by no means the only ones which

may be used, but are in general the most useful for the present purpose. They can easily be demonstrated to be equivalents by direct application of Bartlett's Bisection Theorem.

In Fig. 7(a) a series impedance which is common to both lattice arms can be removed and placed in series with the two output terminals of the network. In Fig. 7(b) a shunt impedance common to both lattice arms can be removed and placed in shunt with each pair of output terminals. Finally in 7(c), a symmetrical lattice which has a series inductor in one of its arms and an inductor in shunt with the other can be transformed to a bridged-T network using a unity turns-ratio transformer with finite inductance and a coupling factor less than unity.

3.3 Reduction Process

It may be helpful to those who have not yet attempted a reduction from lattice to ladder form to give the process in detail. Starting with equations (13) and (14) slightly rewritten for convenience:

$$Z_x = 0.43732 \cdot \frac{jx(0.52893 - x^2)(4 - x^2)}{(0.13223 - x^2)(1.61983 - x^2)} \dots (13a)$$

$$Z_y = 0.37499 \cdot \frac{(0.13223 - x^2)(1 - x^2)(4 - x^2)}{jx(0.52893 - x^2)(1.61983 - x^2)} \dots (14a)$$

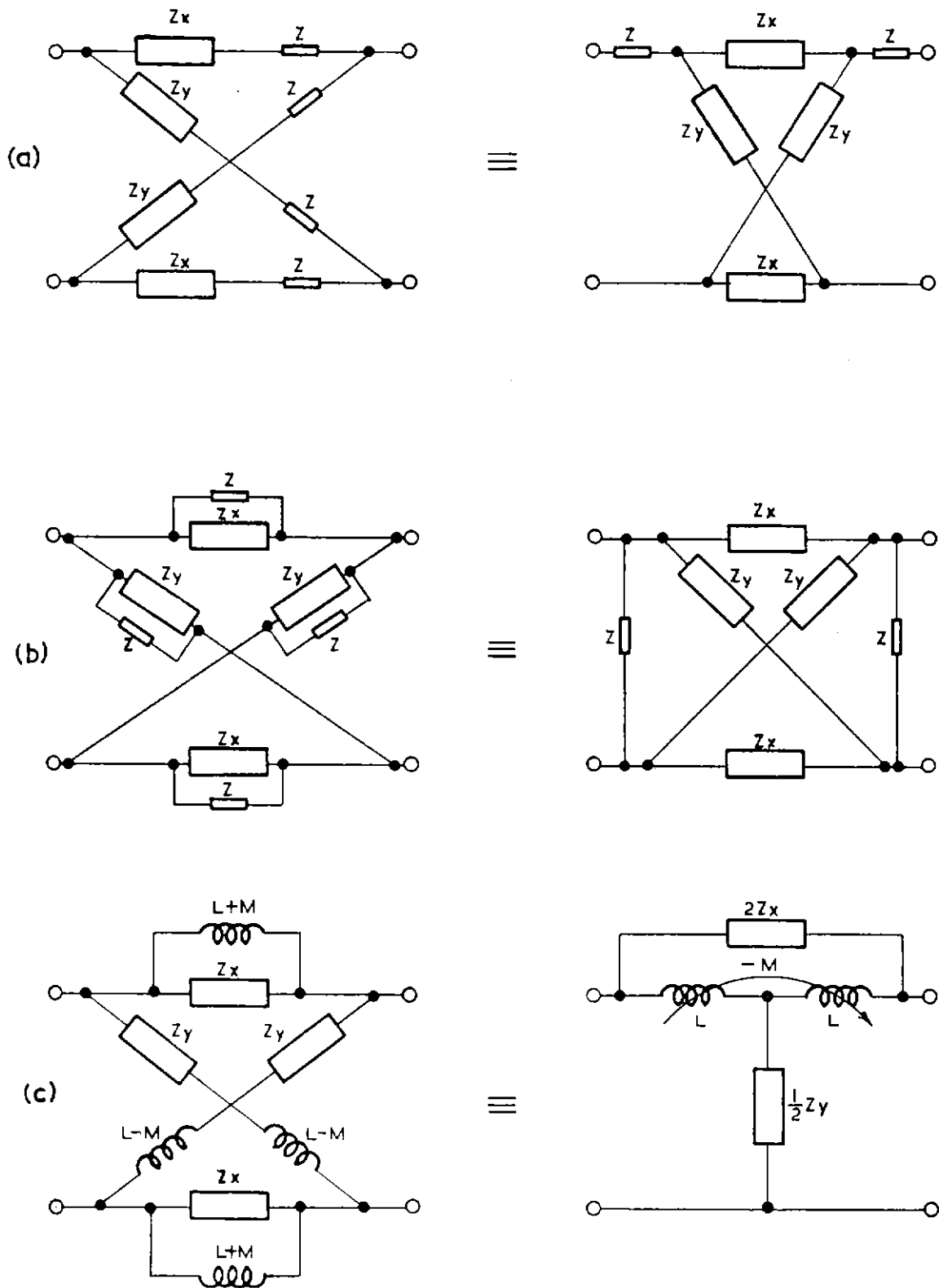


Fig. 7 — Lattice equivalent circuits

It should be mentioned here that the continued taking of differences during the reduction process makes it advisable to work to not less than five significant figures, and the labour can be lightened considerably if a calculating machine is available.

The values of the individual reactance components in Z_a and Z_d must now be obtained by expressing each as the sum of partial fractions.

$$\text{Write } Z_x = Ajx + \frac{Bjx}{0.13223 - x^2} + \frac{Cjx}{1.61983 - x^2} \dots (17)$$

where A, B, C are numerical constants to be determined by identification of (13a) and (17).

To find A make x tend to infinity, when evidently $A = 0.43732$

To find the other coefficients the following device is very useful. For B we multiply both (13a) and (17) by $(0.13223 - x^2)$, so that:

$$0.43732 \cdot \frac{jx(0.52893 - x^2)(4 - x^2)}{1.61983 - x^2} = Ajx(0.13223 - x^2) + Bjx + \frac{Cjx(0.13223 - x^2)}{1.61983 - x^2} \dots (18)$$

Now make x^2 approach 0.13223 , and, in the limit:

$$B = 0.43732 \cdot \frac{(0.52893 - 0.13223)(4 - 0.13223)}{1.61983 - 0.13223} = 0.45106$$

Similarly

$$C = 0.43732 \cdot \frac{(1.61983 - 0.52893)(4 - 1.61983)}{1.61983 - 0.13223} = 0.76332$$

In practice, of course, this device makes it possible for the expressions for these coefficients to be written down by inspection. Inserting the values thus obtained:

$$Z_x = 0.43732jx + \frac{0.45106jx}{0.13223 - x^2} + \frac{0.76332jx}{1.61983 - x^2} \dots (19)$$

which, in agreement with previous findings, represents an inductor in series with two antiresonant circuits.

By an exactly similar process:

$$Z_y = \frac{0.23149}{jx} + 0.37499jx + \frac{0.42155jx}{0.52893 - x^2} + \frac{0.46573jx}{1.61983 - x^2} \dots (20)$$

which evidently agrees with Fig. 5.

Reduction Stage 1. The impedance $\frac{0.46573jx}{1.61983 - x^2}$ is common to both Z_x and Z_y , and so by the equivalent circuit of Fig. 7(a) it can be removed and placed in series with the output terminals of the lattice. The new arms of the lattice are:

$$Z_{x1} = 0.43732jx + \frac{0.45106jx}{0.13223 - x^2} + \frac{0.29759jx}{1.61983 - x^2} \dots (21)$$

$$Z_{y1} = \frac{0.23149}{jx} + 0.37499jx + \frac{0.42155jx}{0.52893 - x^2} \dots (22)$$

Reduction Stage 2. There is also series inductance in each arm, part of which may be taken outside the lattice, but the amount used for this purpose must be decided upon with care. It is known from the scheme of critical frequencies that there is a real frequency of infinite attenuation at $x=2$. Since this does not appear explicitly in (21) and (22), it must be implicit in the equations. The fact that the attenuation peak occurs at a real frequency indicates that there is some real reactance common to each arm which can be used later at a further stage in the reduction, unless too much series inductance is taken out of the arms at this stage. This would result in the common reactance at $x=2$ becoming negative and therefore unusable.

At $x=2$ both Z_{x1} and Z_{y1} have the value $0.39134j$ (this incidentally checks the accuracy of the calculation so far). The most that can be done, therefore, is to remove a series inductance $0.19567jx$, i.e. a reactance of $0.39134j$ at $x=2$, leaving zero reactance at this normalized frequency.

Performing this operation, there is left

$$Z_{x2} = 0.24165jx + \frac{0.45106jx}{0.13223 - x^2} + \frac{0.29759jx}{1.61983 - x^2} \dots (23)$$

$$Z_{y2} = \frac{0.23149}{jx} + 0.17932jx + \frac{0.42155jx}{0.52893 - x^2} \dots (24)$$

Reduction Stage 3. No more can be extracted in the series form, so it is now necessary to see what shunt reactance can be removed. For this purpose the impedance must be inverted into admittance and re-arranged as has been done above for Z_x and Z_y . The process is simple but a little tedious since the roots of the denominator must be found before the individual susceptances are known from the partial-fraction expansion. The results are:

$$Y_{x2} = \frac{0.26065}{jx} + \frac{0.85392jx}{0.85014 - x^2} + \frac{3.02365jx}{4 - x^2} \dots (25)$$

$$Y_{y2} = \frac{0.52169jx}{0.17070 - x^2} + \frac{5.05492jx}{4 - x^2} \dots (26)$$

Now the common admittance $\frac{3.02365jx}{4 - x^2}$, which represents the attenuation peak at $x=2$, can be removed and placed in shunt with the output terminals of the reduced lattice, and there remains:

$$Y_{x3} = \frac{0.26065}{jx} + \frac{0.85392jx}{0.85014 - x^2} \dots (27)$$

$$Y_{y3} = \frac{0.52169jx}{0.17070 - x^2} + \frac{2.03127jx}{4 - x^2} \dots (28)$$

Reduction Stage 4. Y_{x3} and Y_{y3} must now be converted back to the impedance form, giving:

$$Z_{x3} = 0.89723jx + \frac{0.58439jx}{0.19879 - x^2} \dots\dots\dots (29)$$

$$Z_{y3} = 0.39170jx + \frac{0.28058}{jx} + \frac{0.97971jx}{0.95321 - x^2} \dots (30)$$

Now it would be possible to remove series inductance from both Z_{x3} and Z_{y3} , but on the other hand inspection of Y_{x3} shows that its reciprocal Z_{x3} can be put into a form having a shunt inductor while Z_{y3} has a series inductor, and it is known that (see Fig. 7(c)) this fact makes it possible to effect a convenient reduction of the remainder of the lattice to bridged-T form using a transformer with finite inductances and a coupling factor less than unity. Consequently it was decided to stop at this point.

When these inductors have been removed, the residues of the arms become:

$$Z_{x4} = \frac{0.85014 - x^2}{0.85392jx} = \frac{1}{1.0044jx} + 1.1711jx \dots (31)$$

$$Z_{y4} = \frac{0.28058}{jx} + \frac{0.97971jx}{0.95321 - x^2} \dots\dots\dots (32)$$

This completes the actual reduction process; it now remains to calculate the element values.

3.4 Calculation of Element Values

From Stages 1 and 2 of the preceding section it is known that the series arm of the ladder portion, excluding the bridged-T section, consists of an inductor whose generalized reactance is $0.1957jx$, and an antiresonant circuit whose generalized impedance is $\frac{0.4657jx}{1.6198 - x^2}$; these are shown as L_1 and L_2C_2 in Fig. 8.

Taking the inductor first, its reactance is $0.1957jx$ for a filter of unit impedance, and consequently is $0.1957jxR_o$ for an impedance level R_o .

Therefore $0.1957 \cdot \frac{j\omega}{\omega_c} R_o = j\omega L_1$

and $L_1 = 0.1957 \frac{R_o}{\omega_c} \dots\dots\dots (33)$

where f_c is the cut-off frequency of the filter.

The admittance of the antiresonant circuit for an impedance level R_o

$$= \frac{1}{R_o} \cdot \frac{1.6198 - x^2}{0.4657jx} = \frac{1.6198\omega_c}{0.4657j\omega R_o} + \frac{j\omega}{0.4657\omega_c R_o}$$

The first term, because of its form, must represent the susceptance of L_2 , so that

$$L_2 = \frac{0.4657R_o}{1.6198\omega_c} = \frac{0.2875R_o}{\omega_c} \dots\dots\dots (34)$$

The second term must then represent the susceptance of

$$C_2, \text{ giving } C_2 = \frac{1}{0.4657\omega_c R_o} = \frac{2.147}{\omega_c R_o} \dots\dots\dots (35)$$

The shunt arm of the ladder portion is formed by the admittance $\frac{3.0237jx}{4 - x^2}$ removed at Stage 3 of the previous section. This corresponds to a shunt resonant circuit, L_3C_3 of Fig. 8, where by a process similar to that just applied for L_2C_2 ,

$$L_3 = \frac{0.3307R_o}{\omega_c} \dots\dots\dots (36)$$

$$C_3 = \frac{0.7559}{\omega_c R_o} \dots\dots\dots (37)$$

The series arm of the bridged-T section, L_4C_4 , has an impedance twice Z_{x4} , that is $\frac{1}{0.5022jx} + 2.3422jx$, whence

$$L_4 = \frac{2.3422R_o}{\omega_c} \dots\dots\dots (38)$$

$$C_4 = \frac{0.5022}{\omega_c R_o} \dots\dots\dots (39)$$

The shunt arm of the bridge from the equivalent circuit of Fig. 7(c) has one-half the impedance of Z_{y4} , that is

$$\frac{0.1403}{jx} + \frac{0.48985}{0.9532 - x^2}$$

whence

$$L_6 = \frac{0.5139R_o}{\omega_c} \dots\dots\dots (40)$$

$$C_6 = \frac{2.0414}{\omega_c R_o} \dots\dots\dots (41)$$

$$C_7 = \frac{7.1280}{\omega_c R_o} \dots\dots\dots (42)$$

The last remaining element of the filter is the bridge transformer which has equal side inductances L_5 and mutual inductance M . From Fig. 7(c) the shunt inductance removed from Z_{x3} during Stage 4 of Section 4.4 equals $L_5 + M$.

$$\therefore L_5 + M = \frac{3.8366R_o}{\omega_c} \dots\dots\dots (43)$$

and similarly the series inductance removed from Z_{y3} equals $L - M$, so that

$$L_5 - M = \frac{0.3917R_o}{\omega_c} \dots\dots\dots (44)$$

hence

$$L_5 = \frac{2.114R_o}{\omega_c} \dots\dots\dots (45)$$

and

$$M = \frac{1.7224R_o}{\omega_c} \dots\dots\dots (46)$$

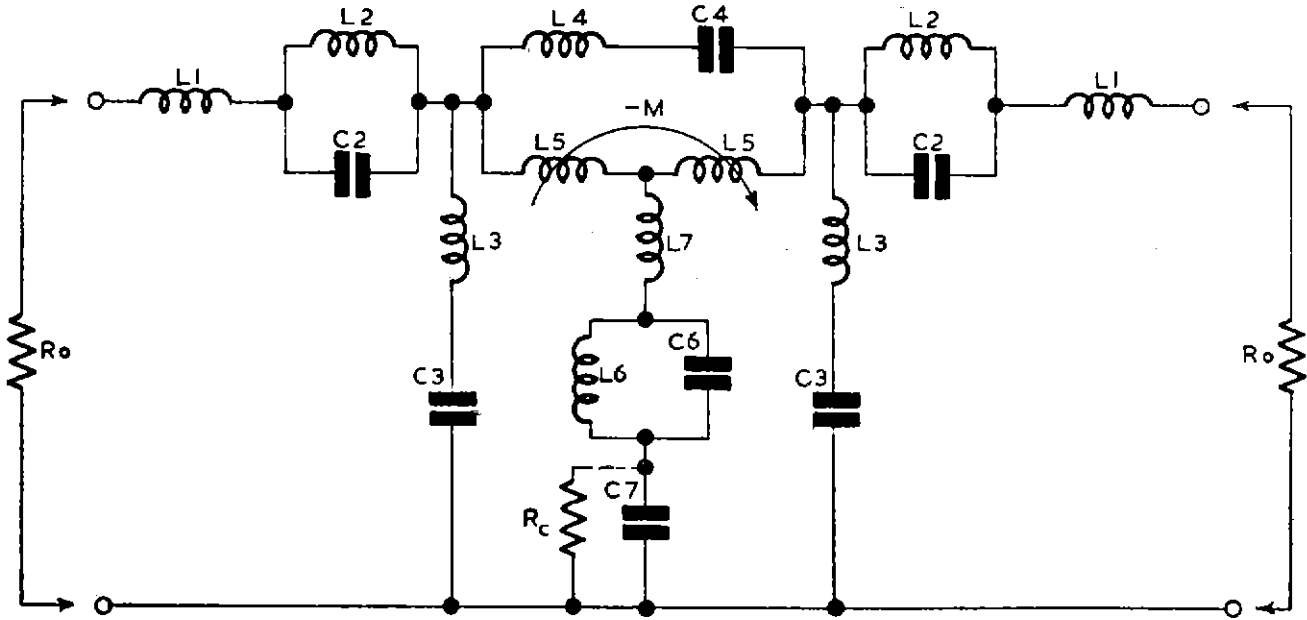


Fig. 8 — Circuit of linear-phase low-pass filter

TABLE I

$L_1 = \frac{0.1957R_o}{\omega_c}$	$L_2 = \frac{0.2875R_o}{\omega_c}$
$L_3 = \frac{0.3307R_o}{\omega_c}$	$L_4 = \frac{2.342R_o}{\omega_c}$
$L_5 = \frac{2.114R_o}{\omega_c}$	$M = \frac{1.722R_o(K=0.815)}{\omega_c}$
$L_6 = \frac{0.5139R_o}{\omega_c}$	$C_2 = \frac{2.147}{\omega_c R_o}$
$C_3 = \frac{0.7559}{\omega_c R_o}$	$C_4 = \frac{0.5022}{\omega_c R_o}$
$C_6 = \frac{2.041}{\omega_c R_o}$	$C_7 = \frac{7.128}{\omega_c R_o}$
$f_{r2} = 1.273f_c$	$f_{r3} = 2.00f_c$
$f_{r4} = 0.922f_c$	$f_{r6} = 0.976f_c$

TABLE II

$L_1 = 0.65\mu H$	$L_2 = 0.95\mu H$
$L_3 = 1.10\mu H$	$L_4 = 7.76\mu H$
$L_5 = 7.0\mu H$	$L_6 = 1.7\mu H$
$L_7 = *$	$C_2 = 1,270pF$
$C_3 = 446pF$	$C_4 = 296pF$
$C_6 = 1,200pF$	$C_7 = 4,200pF$
R_c approx. 520Ω	
$R_o = 75\Omega$	$f_c = 3.6$ Mc/s
$f_{r2} = 4.58$ Mc/s	$f_{r3} = 7.20$ Mc/s
$f_{r4} = 3.32$ Mc/s	$f_{r6} = 3.51$ Mc/s

* Chosen to give the correct value of M with the transformer used.

From (45) and (46) the coupling factor is 0.8147, and the two halves are connected in series-aiding as shown in Fig. 7(c).

The element values calculated above are tabulated in Table I. Table II gives the element values for the chosen cut-off frequency of 3.6 Mc/s and an impedance of 75 ohms; it is clear that they are all of a quite reasonable order of magnitude.

4. Practical Considerations

4.1 Components

The bridge transformer always presents especial difficulties in filters employing bridged-T sections. First of all an exact value of mutual inductance is required, since it is used as a reactive element of the filter, and it is not usually practicable to achieve this. The device normally resorted to

whenever possible is to over-couple the transformer somewhat, which has the effect of producing a more negative value of mutual inductance than required, and to add an adjustable self-inductance in series with the shunt arm of the bridge so that the excess negative inductance from the mutual coupling can be neutralized very precisely. In the present case the coupling coefficient required is such that a small degree of overcoupling can be achieved without any difficulty by using a totally enclosed 'pot' type dust core.

Unfortunately, high coupling coefficients involve relatively high stray capacitances across the windings and low values of Q , and a good deal of ingenuity may be required to design the transformer in certain cases. Where the Q cannot be made high enough to avoid degrading the filter performance, it is often possible to resort to resistance-compensation (see Section 4.4). In any case, a method of winding must be adopted which leads to consistent values of these quantities whether they are desired or not.

The inductors and capacitors must also have as high a Q as possible, particularly in the cut-off region where the

effects of dissipation are always marked. Since the loss at the frequencies of (ideally) infinite attenuation is not very important with this particular filter, there is no need to strive for exceptionally high Q 's in that region.

The self-capacitance of the inductors and the series inductance of the capacitors must be kept to a minimum, otherwise, even if no actual resonance occurs within the band, the variation of effective inductance or capacitance with frequency can give considerable trouble.

For a filter of the type considered, where a high degree of reproducibility is required, and where the capacitance values are large compared with the stray capacitances, it is not unreasonable to call for fixed capacitors with a tolerance of ± 1 per cent. The inductors are of a range of values such that they can be conveniently wound on dust cores with adjustable slugs. The alignment of the filter is thereby made considerably easier since the capacitors can be assumed to be exact, and it is then only necessary to resonate each individual circuit to the calculated frequency by means of its inductor.

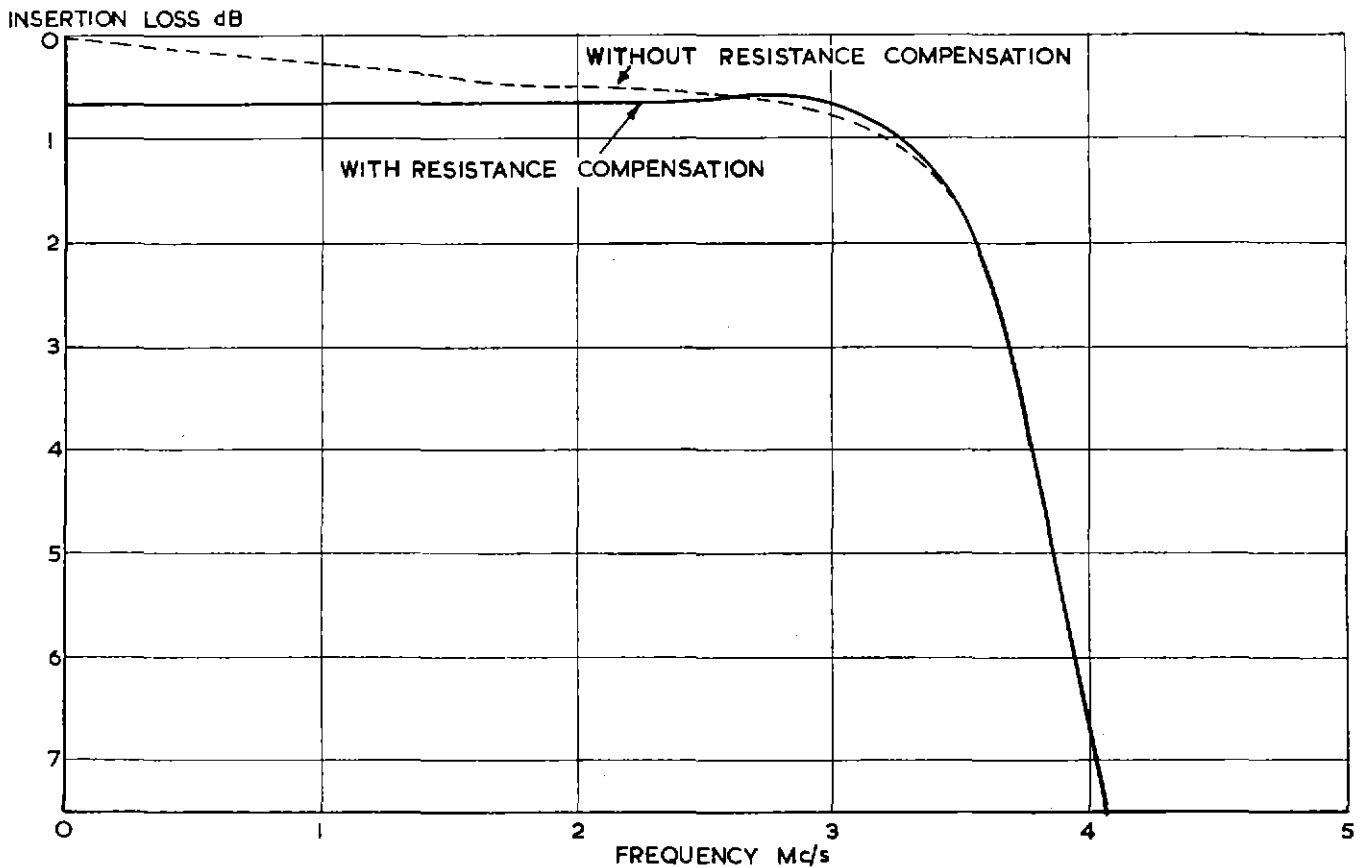


Fig. 9 — Pass-band of linear-phase low-pass filter No. 1 showing effect of resistance compensation

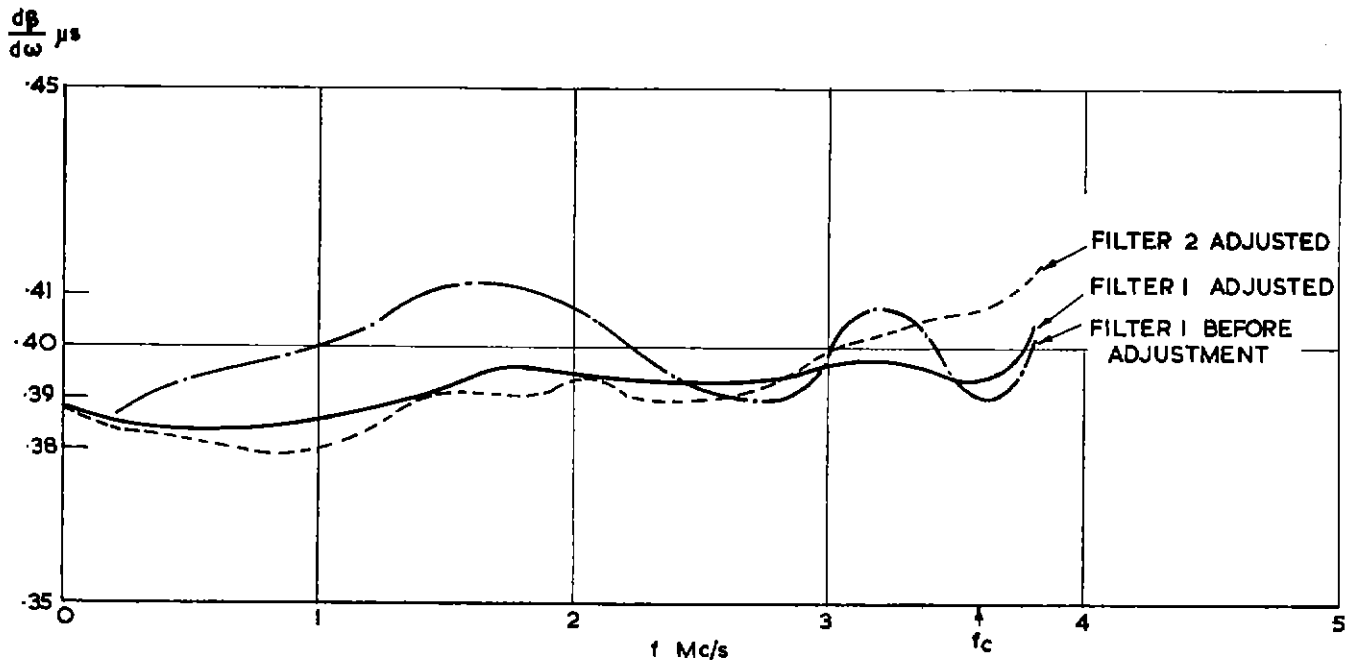


Fig. 10 — Linear-phase low-pass filters — group-delay measurements

4.2 Mechanical

By making use of 6-mm coil formers designed for mounting in small, rectangular section aluminium screening cans, it was found possible to compress the filter into a copper can measuring 6 in. \times 2 $\frac{1}{8}$ in. \times 2 $\frac{1}{8}$ in. externally, without any sacrifice of performance. Fig. 11 clearly shows how the components are mounted on a copper plate, which is shown in position in its screening can in Fig. 12. The input and output connections are made by means of 75-ohm cables, and the retaining clamp for one of these can be seen in Fig. 12.

In deciding upon the layout of the components, the obvious considerations were kept in mind with respect to lengths of leads and reduction of stray capacitance to case to a minimum. The latter is of special importance at points such as the junction of L_4 and C_4 ; it can be made negligible in effect in the shunt arms by connecting C_3 in the earthy side as shown in Fig. 8, so that the capacitance to case of L_3 falls across C_3 .

In order to prevent too much disturbance to the wiring during the alignment procedure, use was made of very low capacitance stand-off tags so that the various individual resonant circuits could be more readily isolated for individual adjustment.

4.3 Alignment

Before assembly and wiring the capacitances were checked and all inductors, in their screening cans, were set on a low-frequency bridge to the nominal value. The bridge transformer L_5 with its associated inductor L_7 were adjusted together to give the required values of side inductance

and mutual inductance; at the same time a check was made on the balance of the two halves of the winding. This ensured that, when wired, the filter was already in approximate alignment.

The precise alignment of each circuit was performed with the aid of a stable signal generator, set by means of a quartz crystal Frequency Checking Unit, and a high-gain radio receiver provided with a meter reading the signal diode current.

Although the filter is by no means 'fussy' with respect to hand capacitance or proximity to other objects, the final adjustments were made with it mounted in a dummy can. This is the same as the normal can but is provided with holes for access to the coil slugs.

The circuits L_2C_2 and L_3C_3 could be set very simply and without disturbing the wiring since L_2C_2 are responsible for the first f_{∞} at 4.58 Mc/s, and L_3C_3 for the second at 7.2 Mc/s. The oscillator was connected to the input of the filter and set to 4.58 Mc/s, and the receiver input was connected to the output of the filter and tuned to the oscillator frequency. Circuits L_2C_2 were then adjusted by means of the inductor slugs until the loss through the network was a maximum. Circuits L_3C_3 were adjusted in a similar fashion.

The remaining circuits were resonated in the following way. A pair of moderately high resistors was connected between the output of the oscillator and the receiver input; the most suitable value of resistance was found by experiment. The circuit to be resonated was disconnected from the remainder of the filter, although left in position, and connected between the junction of these resistors and

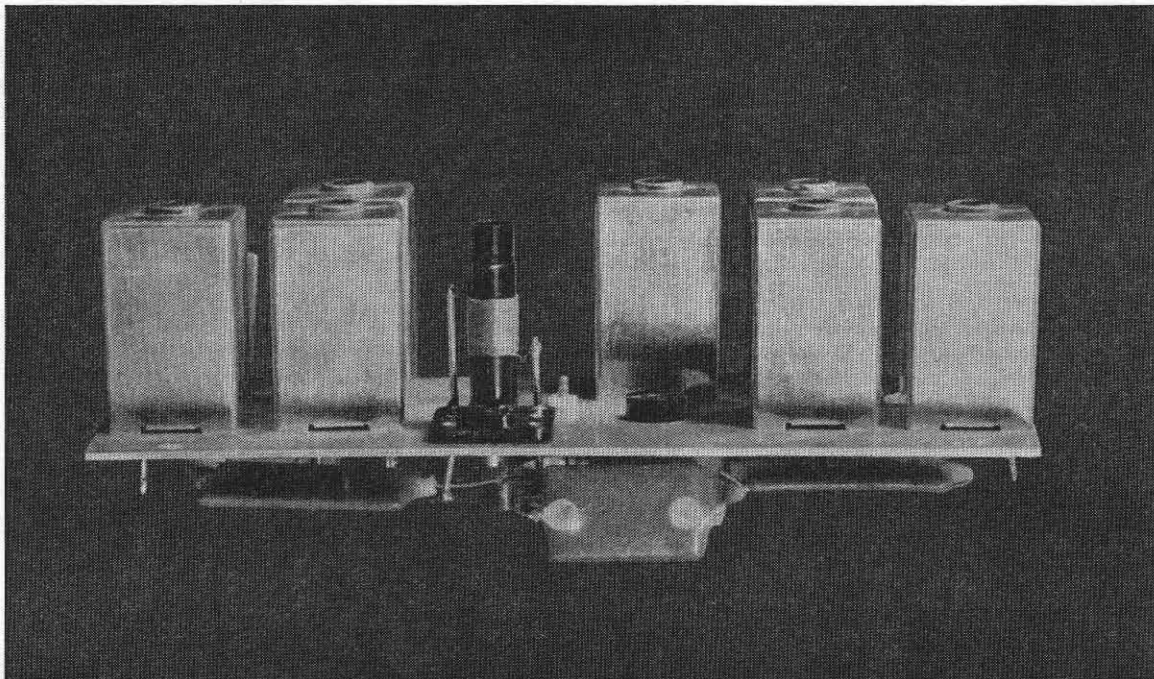


Fig. 11 — Filter removed from can

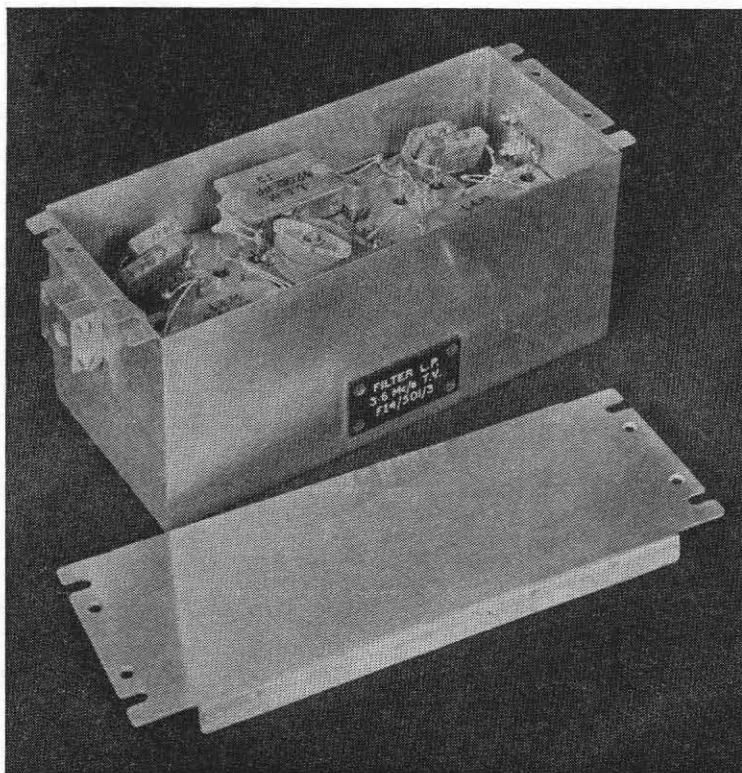


Fig. 12 — Filter mounted in can

earth. It was then set by turning the coil slug until either a minimum or maximum was obtained on the receiver meter according to whether the circuit was in resonance or anti-resonance.

4.4 Resistance Compensation

After the alignment procedure described in the foregoing section, the insertion loss of the filter was measured between good 75-ohm terminations, and the curve (a) of Fig. 9 was obtained. This agrees very well with the calculated curve except for a drop of about 0.7 dB up to 3 Mc/s which was diagnosed as being mostly due to a combination of increasing dissipation towards the higher frequencies from the bridge transformer and the bridge series arm.

The author has previously found that an extension of Landon's method of resistance compensation⁽⁵⁾ is often very effective in such a case. This normally is applied at a single or a pair of conjugate frequencies of infinite attenuation where the calculation is very simple, and as high a degree of compensation can be achieved as required or the stability of the circuit components allows.

It can easily be shown by calculation, or demonstrated by a simple application of Bartlett's Bisection Theorem, that at one given frequency a resistance in the series or bridge arms of a bridged-T network can be compensated by the correct value of resistor inserted in the shunt arm, or vice versa. In terms of the equivalent lattice, at the frequency considered, the arms can be manipulated in such a way that the same value of resistor appears either in series with or in shunt with each arm and can therefore be taken outside the lattice itself (see Fig. 7(a) and 7(b)). Special configurations occur where the compensation is exact for all frequencies.

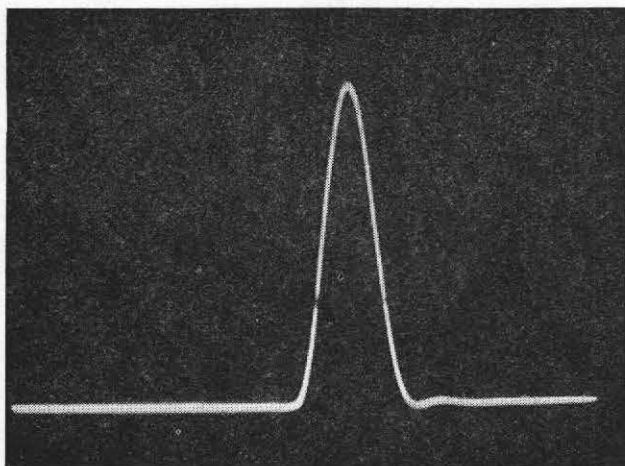
In the present instance it was evident that the compensation could not be exact, if only because of the variation with frequency of the effective resistance component in the series arm, but on the other hand the amount to be corrected is so small that a quite approximate compensation would be adequate.

An examination of the circuit suggested that a resistor in parallel with C_7 would be effective, and in fact a value of 520 ohms was found to give an attenuation response up to the cut-off frequency negligibly different from the calculated response, as shown in the curves of Fig. 9, except for an expected increase in the pass-band loss to 0.6 dB. An experiment with three models of the filter demonstrated that this result could be achieved by using random samples of 520 ohms \pm 2 per cent resistors, although, of course, there is always the possibility that in later models changes such as dust-cores from a different batch or slight variations in the manner of winding the coils might make values outside that narrow range necessary.

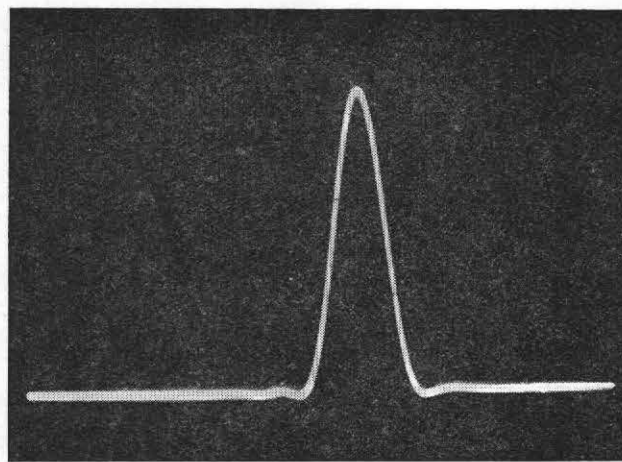
4.5 Improvement of Group-Delay Characteristic

It might be expected that, very broadly speaking, the portion of the filter which has been reduced to simple ladder form represents the minimum phase-shift, and the remainder the excess phase-shift part; that is, very roughly, the first part is the filter and the second the phase corrector. In practice this is often, but not invariably, the case.

This fact suggested that it might be possible to make use of a sine-squared pulse technique^(6,7) to improve somewhat the group-delay response—already very good—by an empirical modification of the elements in the bridged-T section.

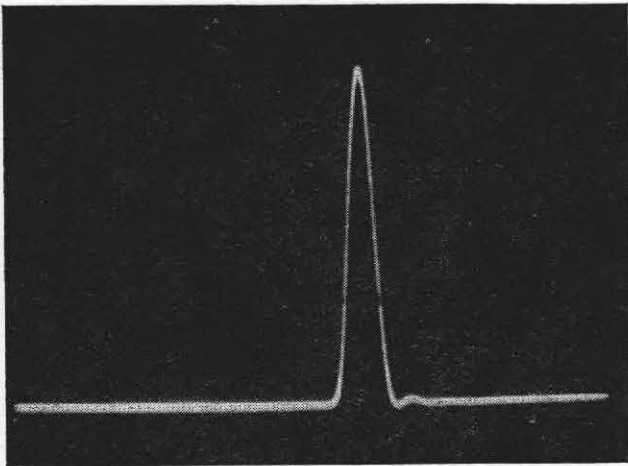


1. '2T' \sin^2 pulse at the input of filter

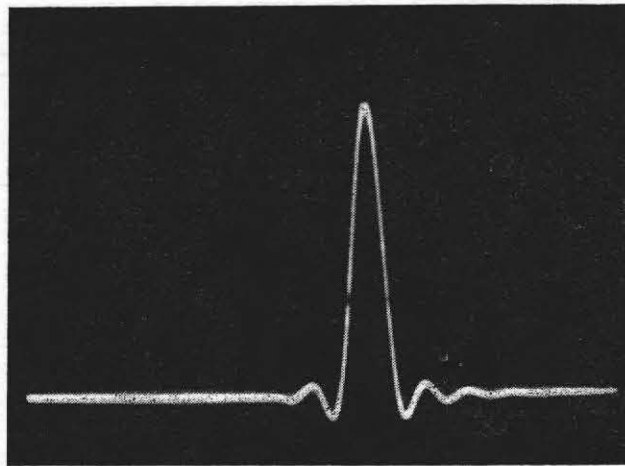


2. '2T' \sin^2 pulse at the output of filter

Fig. 13 — '2T' sine-squared pulse response



3. 'T' \sin^2 pulse at the input of filter



4. 'T' \sin^2 pulse at the output of filter

Fig. 14 — 'T' sine-squared pulse response

The response of a filter aligned as previously described was measured. It was then inserted between two small 75-ohm pads to ensure a good termination, and a 0.167- μ s sine-squared pulse was sent through the filter and examined on a high-grade oscilloscope.

It was found that a quite large range of adjustment of L_5 and L_7 varied the phase with no perceptible change in the amplitude response, so they were adjusted until optimum symmetry of the leading and lagging transients caused by the cut-off of the filter was obtained, taking into account the slight initial asymmetry of the original pulse. These transient 'rings' are due primarily to the reduction of the width of the pulse spectrum, and the presence of the anticipatory transient arises from the non 'minimum-phase-shift' character of the network. Now pure amplitude distortion of a waveform produces wholly symmetrical distortion, while pure phase distortion produces completely skew-symmetrical distortion. Hence, if the asymmetry of the output waveform is made as small as possible, the residual phase distortion will be minimized. Accordingly the 'T' sine-squared pulse response was carefully observed on a cathode ray oscilloscope and L_5 and L_7 were varied until the optimum condition of symmetry was reached. The filter was then re-measured, and the two curves are shown superimposed in Fig. 10. Fig. 14 shows the input and output 'T' pulses for this condition, and the symmetry of the output pulse should be noted. The magnitudes of the leading and lagging transients are due to the slope of the attenuation characteristic in the cut-off region.

The improvement in the group-delay curve produced by this adjustment is not large in terms of total spread, but the oscillations are reduced in amplitude and the major

variation takes place over a wider interval. The sensitivity of the pulse to very small phase errors encouraged the belief that the method might be used as a means of setting the group-delay response precisely to this optimum condition during manufacture. Accordingly, a second filter was aligned and readjusted in a completely similar manner, and the measured curve is also shown in Fig. 10. It will be noticed that up to 3 Mc/s the difference between the curves is extremely small, in fact roughly of the order of the measurement accuracy; above 3 Mc/s the difference is still quite small, and in any case it occurs in a part of the frequency range where it is of less consequence.

On the basis of these results it was judged that the sine-squared pulse method is not only of great practical use for checking the alignment of a filter designed as described above, but also makes it possible to effect a useful further improvement in its performance in a repeatable manner.

5. References

1. Mayer, H. F., **The Damping of Filters in the Transmission Region**, *Elektrische Nachrichten-technik*, October 1925.
2. Bode, H. W. and Dietzold, R. L., **Ideal Wave Filters**, *Bell System Technical Journal*, April 1935.
3. Bode, H. W., **A General Theory of Electric Wave Filters**, *Massachusetts Institute of Technology Journal of Mathematics and Physics*, November 1934.
4. Floyd, C. F. and Corke, R. L., **The Design of Linear-phase Low-pass Filters**, *Proc. I.E.E.*, Vol. 99, Part IIIA, 1952.
5. Landon, V., **M-derived Band Filters with Resistance Cancellation**, *Proc. I.R.E.*, October 1936.
6. Macdiarmid, I. F., **A Testing Pulse for Television Links**, *Proc. I.E.E.*, Vol. 99, Part IIIA, 1952, p. 436.
7. Lewis, W. N., **Waveform Responses of Television Links**, *Proc. I.E.E.*, Vol. 101, Part III, 1954, p. 258.

NOTE ON RANDOM FLUCTUATION NOISE IN IMAGE ORTHICON CAMERA TUBES

by

R. D. A. MAURICE, Ing.-Dr, Ing.E.S.E., A.M.I.E.E.
(Research Department, BBC Engineering Division)

The image orthicon television camera tube is being used ever more widely, particularly for broadcasting, and recent unpublished measurements have confirmed the existence of a feature of the noise produced by this tube which was not realized at the time of publication of BBC Engineering Division Monograph No. 3, 'The Visibility of Noise in Television'. In Part I, 'The Visibility of Noise over the Grey Scale', it was stated in Section 6 that 'the noise . . . is proportional to the half-power of the return beam current.' It is now thought that this is not correct and that, in fact, the noise is proportional to the half-power of the incident or scanning-beam current. This will make an observable difference to the distribution of noise over the grey scale.

A reasonable explanation is quite simple and can be stated as follows:

- Let i_b = scanning-beam current incident on the tube target
- i_s = signal current abstracted from the incident scanning-beam and left as a charge pattern on the target
- $i_r = i_b - i_s$, the return beam which becomes amplified by the secondary-emission multiplier dynodes and gives rise to the output current from the tube
- $m = i_s/i_b$, the beam modulation index assumed to be proportional to i_s , except at very low levels of the 'potential swing' which will not be considered here
- e = the charge of an electron
- Δf = channel video bandwidth

The noise power in the return beam will be $2ei_s\Delta f$, in accordance with the well-known expression for the total power of random velocity fluctuations in an electron beam. Similarly, the noise power in the signal current will be $2ei_s\Delta f$. The random fluctuations represented by this power will be imprinted on the target during each scan. The noise power in the return beam will thus be the sum of the intrinsic noise power of the return beam itself and the noise power due to the signal current 'read' off the target during a subsequent scan (third scan in the case of interlaced television). If we assume that movement in the scene being televised is sufficiently slow for alternate scans to be taken as identical, we may write:

$$N^2 = 2ei_s\Delta f + 2ei_s\Delta f \\ = 2ei_b\Delta f \dots\dots\dots (1)$$

where N^2 is the total noise power appearing in the return beam and, if the multiplier section of the tube contributes no further noise, it represents the noise power in the output signal from the tube.

We see that the noise output is derived entirely from the incident scanning-beam and since the camera tube is so operated that the incident-beam current is adjusted once and for all to discharge those portions of the target which receive a charge due to the brightest parts of the scene, the noise power is dependent upon the peak-white brightness and it is thus independent of the actual signal level being transmitted at any given instant.

Of course, the signal output, S , from the camera tube is proportional to the signal current, $i_s = mi_b$. The signal-to-r.m.s. noise ratio at the camera-tube output is therefore

$$S/N \propto m\sqrt{i_b/2e\Delta f} \dots\dots\dots (2)$$

It would be of value to compare the signal-to-noise ratios of the various types of image orthicon camera tube in use today, but, unfortunately, to do this thoroughly would require an understanding of the functioning of these tubes that the writer does not possess.

In the case of tubes having a relatively large separation (greater than a picture element diameter) between the target and the secondary-emission collector mesh, for which gamma correction ($\gamma=2/5$) circuits are unnecessary, Section I and Fig. 3, Part I, of the above-mentioned monograph show that the visual sensation of the noise will remain independent of the brightness distribution of the scene being received and displayed.

For tubes with a close-spaced (less than a picture element diameter) target-and-mesh assembly, the passage from linear transfer of light input to current output (with no electron redistribution effects) to virtual saturation, at which the image transfer relies entirely on electron redistribution, is abrupt. Such tubes are operated mainly over the linear region of the transfer characteristic and gamma correction is required. A treatment similar to that undertaken in Section 3 and Fig. 4, Part I, of the same monograph shows that in this case the noise sensation rises towards the darker tones in the displayed image and is, in fact, proportional to $B^{-3/5}$ where B is the instantaneous brightness being displayed.

In fact, for the 'wide-spaced' tube, we find that the ratio of peak-white signal to r.m.s. noise, measured in visual sensation units, is proportional to $\sqrt{i_{bw}}$, where i_{bw} is the incident scanning-beam current for the 'wide-spaced'

tube. For the 'close-spaced' tube fitted with gamma ($\gamma=2/5$) correction, the same ratio is proportional to $(5/2)\sqrt{i_{bc}}(B/B_p)^{3/5}$, where i_{bc} is the incident scanning beam current for the 'close-spaced' tube and B/B_p is the ratio of the brightness of any given part of the scene to that of the brightest part. The assumptions underlying these statements are that the signal-to-noise ratios are large, that the beam modulation indices are identical and that $\gamma=2/5$.

These assumptions undoubtedly lead to considerable over-simplification, but what may be said with reasonable certitude is that the noise levels are in inverse ratio to the square-roots of the incident beam currents and that the distribution of the noise over the grey scale, in terms of visual sensation units, is uniform for the 'wide-spaced' tube (in the absence of gamma correction) and rises in the darker tones approximately in accordance with a three-fifths power law for the 'close-spaced' tube (in the presence of gamma correction).

Comparisons between tubes having different target-to-mesh separations and targets of different areas are difficult to establish theoretically, as was pointed out to the writer by his colleague, Mr H. G. Anstey.* Further complications

are introduced by the use of a 'field' mesh on the scanning-beam side of the target as Mr W. E. Turk† has warned. Nevertheless, in view of the inaccuracy of the treatment of the image orthicon camera tube in the above-mentioned monograph and of the fact that although it can be deduced from American⁽¹⁾ and British⁽²⁾ publications that the noise power of the output signal from these tubes is proportional to the incident scanning-beam current rather than to the signal current alone, it is felt that there may be many who have not realized the full significance of the independence of the noise from the actual value of grey tone being transmitted at any given instant. In this respect, image orthicons do not differ from camera tubes in which the main contribution to noise is in the head amplifier.

References

1. Rose, A., Weimer, P. K., Law, H. B., **The Image Orthicon—A Sensitive Television Pickup Tube**. Proc. I.R.E., Vol. 34, No. 7, July 1946.
 2. Bedford, L. H., **Television Camera Tubes**. Wireless Engineer, Vol. XXVIII, No. 328, January 1951.
- * Operations and Maintenance Department (Television), BBC.
† English Electric Valve Company.

Published by the British Broadcasting Corporation, 35 Marylebone High Street, London, W. 1
Printed on Basingwerk Parchment in Times New Roman by The Broadwater Press Ltd, Welwyn
Garden City, Herts. *No. 3798*